JOURNAL OF MATERIALS SCIENCE 28 (1993) 3653–3660

Acoustic microscopy of ceramic-fibre composites

Part III *Metal-matrix composites*

C. W. LAWRENCE, G. A. D. BRIGGS
Department of Materials, University of Oxford, Parks Road, Oxford, OX1 3PH, UK
C. B. SCRUBY
AEA Technology, Harwell Laboratory, Oxon, OX11 0RA, UK

Scanning acoustic microscopy (SAM) has been used to study metal matrix composites (MMCs) reinforced with silicon-carbide monofilaments. For most of the specimens the matrix was Ti–6Al–4V, but Ti_3Al and 6061 Al matrices were also examined. The titanium-matrix specimens were subjected to a range of thermal ageing treatments to investigate potential in-service degradation. The main effect was progressive deterioration of the fibre–matrix interface. In the as-received material the carbon-rich coating protected the SiC by forming a reaction layer with the titanium. As a result of ageing, the reaction layer was penetrated adjacent to the β-phase titanium grains. More extensive ageing caused the carbon-rich coating to degrade and eventually disappear. The final stage of deterioration was direct attack on the SiC. Cracks and porosity between fibres were observed in some specimens, probably due to poor diffusion bonding during fabrication. Fine radial microcracks were observed in an annular region inside the mid-radius of some fibres; they are believed to be a consequence of stress relief during thermal ageing. These cracks could not be observed optically. The extra sensitivity of acoustic microscopy is due to the reflection of Rayleigh waves by tight closed cracks.

1. Introduction

Metal matrix composites (MMCs) have been developed for their superior specific mechanical properties compared with unreinforced metals for the medium temperature range 300–600 °C [1, 2, 3]. Although polymer-matrix composites with glass and carbon-fibre reinforcement have been great successes as light strong materials; they are limited to temperatures below 350 °C. The replacement of the polymer matrix with a metal matrix also gives better resistance to environmental degradation and better shear strength, with a smaller weight penalty than using a pure metal. Glass and ceramic matrix composites (CMCs) which were studied in Parts I and II [4, 5] are under development for even higher temperature applications than MMCs.

One MMC with potential for high-temperature applications (e.g. gas turbine components) where weight, strength and stiffness are all important factors uses titanium alloyed with 6% aluminium and 4% vanadium (Ti–6Al–4V) as the matrix and silicon-carbide monofilaments as reinforcement. In this composite the function of the matrix is to provide ductility and toughness while the fibres give extra strength, rigidity and creep resistance. A good interface between the matrix and the fibres is essential to ensure that tensile stresses are adequately transferred to the fibres. It is of crucial importance to be able to determine how the composite performs during typical service conditions. These can readily be simulated by various thermal ageing treatments. While there is interest in being able to monitor all aspects of material degradation, the condition of the fibre–matrix interface is of paramount importance to the strength and integrity of the composite. Thus the main purpose of this study is to investigate the degradation of the SiC-reinforced Ti–6Al–4V composite as a function of thermal ageing. As in Parts I and II, the main technique is acoustic microscopy, chosen for its sensitivity to changes in elastic properties caused by variations in microstructure and for its ability to image very small defects such as cracks [6]. All the micrographs were obtained with a scanning acoustic microscope supplied by Leica (Wetzlar, Germany). Further details of this type of instrument and experimental procedures for obtaining optimum acoustic images can be found in [7, 8]. Quantitative measurements of ultrasonic velocity were made using both point-focus-beam and line-focus-beam [9] microscopy.

2. Materials and specimen preparation

The main material studied was a proprietary MMC manufactured by Textron and supplied by Rolls–Royce Plc, Derby. The matrix was a Ti–6Al–4V titanium alloy (6% aluminium, 4% vanadium, balance

0022–2461

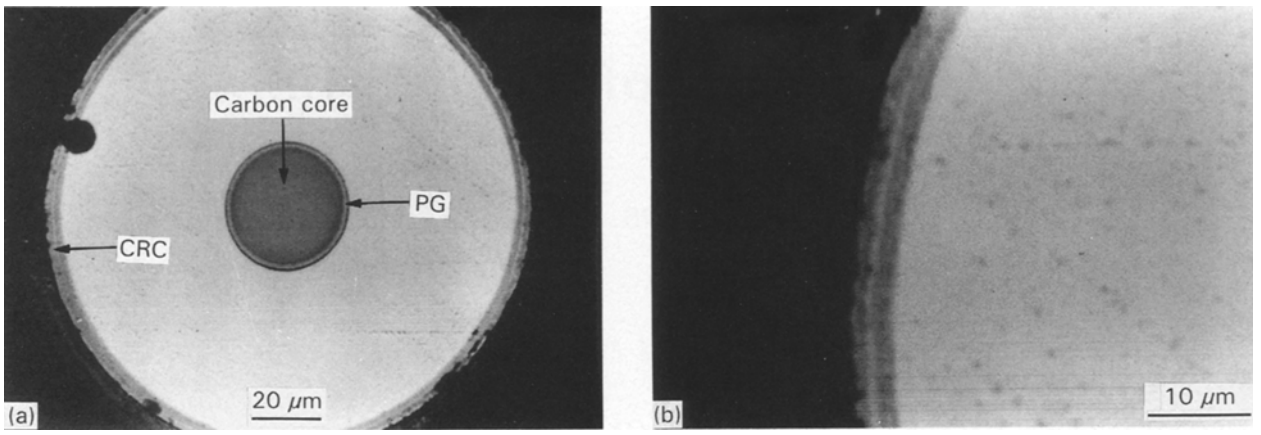

Figure 1 (a) Acoustic micrograph (1.9 GHz, $z = 0$ μm) of a Textron SCS-6 SiC monofilament mounted in epoxy resin: PG, pyrolitic graphite layer; CRC, carbon-rich coatings. (b) Enlargment of a carbon-rich coating.

titanium) which was reinforced by parallel silicon-carbide monofilaments. This material is manufactured from layers of a prepreg of parallel silicon-carbide monofilaments held together in a thin sheet by a polymer binder, alternating with thin foils (50–100 μm) of the titanium alloy. After removing the binder by vacuum heating to 400–500 °C, the composite is consolidated by hot pressing to 105 MPa at 925 °C for 45 min. The specimens used for this study were all eight-ply material. Optical and acoustic microscopic examination of the as-fabricated material revealed a reasonably even distribution of monofilaments and an average volume fraction of 0.36 [10].

The reinforcement was Textron (formerly Avco) SCS-6 silicon-carbide monofilaments. Fig. 1a, an acoustic micrograph of a single monofilament shows the carbon core, pyrolitic graphite layer, silicon carbide and carbon-rich coatings. The diameter was measured to be 143 μm, in agreement with the manufacturer's figure. Closer examination (Fig. 1b) revealed the carbon-rich coating consisted of at least three layers. The middle layer (lightest contrast) was 1 μm thick, and the inner and outer layer were both 1.7 μm, to give a total thickness of 4.5 μm.

One specimen was examined in the as-fabricated condition, while the remaining four specimens were studied after a range of heat treatments carried out by Rolls–Royce. Their purpose was to simulate potential service conditions and investigate degradation of the material. Ageing temperatures of 450 °C and 600 °C were chosen, and the duration was either 500 or 1000 h (Table I).

All the specimens were mounted in transverse section and polished for optical metallography. However, because they had been prepared using polishing cloths, there was a certain amount of relief polishing around the monofilaments. These tended to stand proud, the matrix sloping away from the interface. The specimens were not repolished for fear of damage to the fibre–matrix interface. The size of the monofilaments ensured that they themselves were flat enough not to perturb the acoustic image. However, extra care was needed to avoid topographical effects when interpreting acoustic contrast from matrix regions adjacent to the fibres.

TABLE I Details of the heat treatment of the specimens

Specimen	Temperature (°C)	Duration (h)
1		
2	450	500
3	450	1000
4	600	500
5	600	1000

A specimen of α-titanium aluminide (Ti_3Al) reinforced with Textron SCS-6 SiC monofilaments was also examined in the as-fabricated condition by acoustic microscopy. The specimen was supplied with the same surface condition as the five specimens above, and there was no need for further polishing. A specimen of 6061 aluminium alloy (Al–1.0 Mg–0.6 Si–0.3 Cu–0.2 Cr) reinforced with SiC monofilaments was also briefly examined in the acoustic microscope. This material is of additional interest because it uses a more recent variant of the Textron SiC monofilament, SCS-10, although this particular fibre was developed primarily for use with titanium-based matrices, having a 3 μm graded coating.

3. Results

3.1. As-fabricated material

Acoustic microscopy of the as-fabricated material revealed an approximately even distribution of SiC monofilaments in a Ti–6Al–4V matrix with no obvious signs of fabrication damage. The acoustic image of a typical monofilament (Fig. 2a) appears to be slightly stretched vertically, this is due to a temporary scanning fault in the microscope. There are a number of features in common with the virgin monofilament of Fig. 1a. Thus a 33 μm carbon core is still visible together with a surrounding 1.3 μm layer of pyrolitic graphite. The irregularities in the graphite–SiC interface are indicative of a chemical reaction between these materials.

Moving further outwards, there are microstructural features in the silicon carbide that were not visible in Fig. 1. Thus there is a band extending out to the mid-radius (MR) boundary at 22 μm. The microstructure is

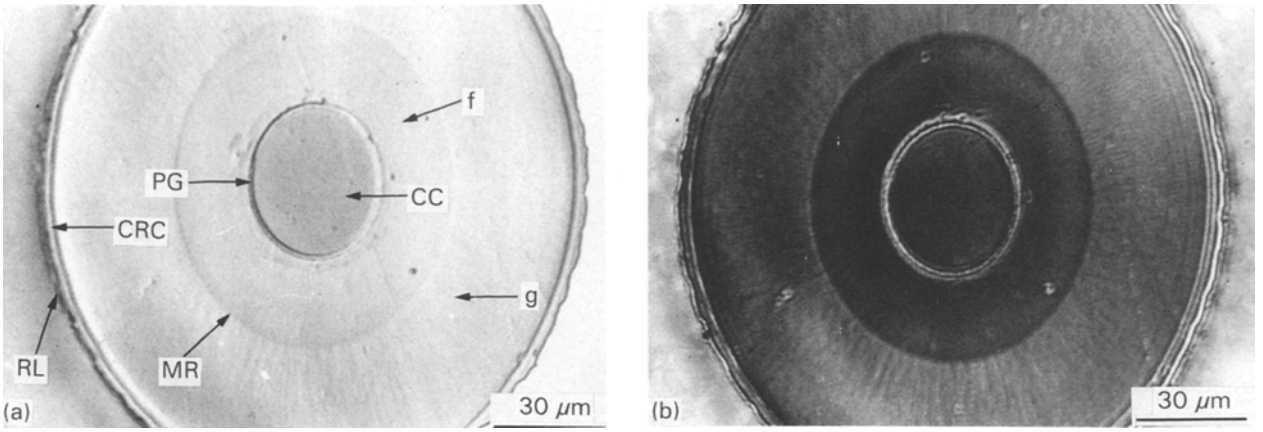

Figure 2 Acoustic image (1.9 GHz) of the microstructure of a SiC monofilament in as-fabricated specimen 1 at: (a) $z = 0$ μm, and (b) $z = -0.5$ μm. CC, carbon core; PG, pyrolitic graphite layer; CRC, carbon-rich coatings; RL, reaction layer; MR, mid-radius boundary between finer-grained, f, and coarser-grained, g, SiC. The vertical magnification is slightly greater than the horizontal magnification.

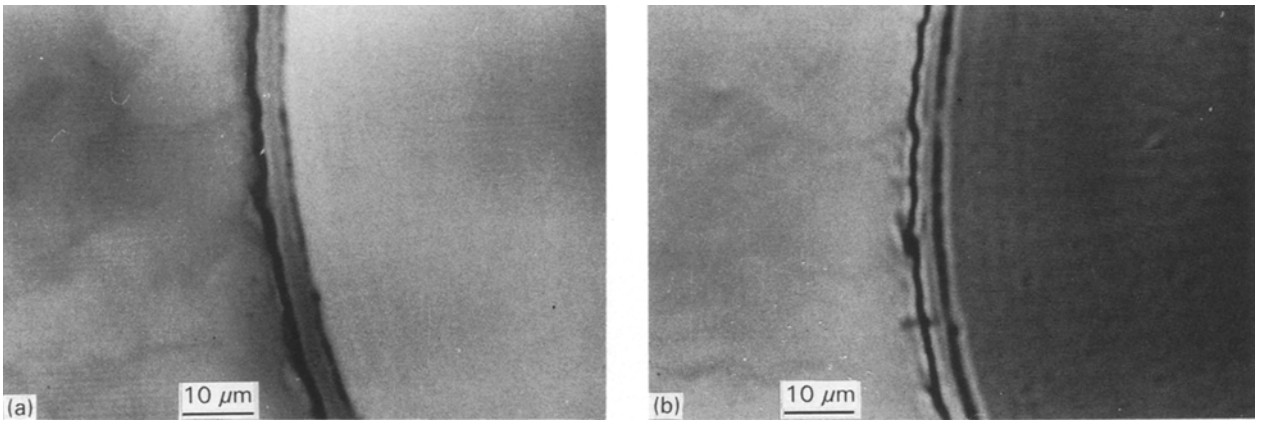

Figure 3 Higher-magnification acoustic image (1.9 GHz) of the interfacial region between the Ti–6Al–4V matrix and the SiC monofilament in as-fabricated specimen 1 at:(a) $z = 0$ μm, and (b) $z = -1.0$ μm. Note the contrast variations corresponding to three distinct layers within the carbon-rich coating.

known to consist of columnar grains radiating out from the centre of the monofilament. When a negative defocus is selected (Fig. 2b) Rayleigh waves are generated which are sensitive to this microstructure, so that the contrast difference between the two regions is enhanced. Within the band, fine-grained silicon carbide is observed (f), whereas outside the MR boundary the silicon carbide is coarser (g). This observation is consistent with changes in concentration of the reactants in the chemical-vapour-deposition chamber. The resolution in the coarser region is sufficient to estimate the grain length as 3–4 μm, which is in good agreement with results in the literature [11].

The carbon-rich coating surrounding the SiC is partially replaced by a reaction layer (Fig. 2a). Higher-magnification acoustic micrographs (Fig. 3) show at least three thin regions of varying contrast that separate the fibre from the matrix. These data suggest that certainly the inner layer and possibly also the middle layer of the carbon-rich coating prior to fabrication (Fig. 1) remain intact, whereas the outer carbon layer has reacted with the titanium of the matrix. The structure of this layer as deduced from acoustic microscopy is shown schematically in Fig. 4. The reaction layer is likely to consist mainly of TiC; it is also

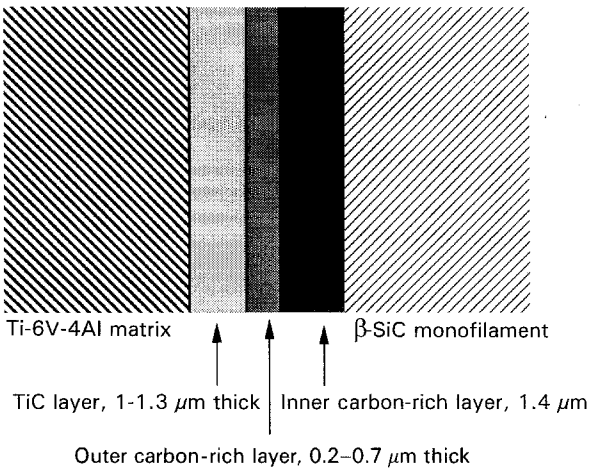

Figure 4 Schematic diagram of interfacial structure for as-fabricated specimen 1 observed in Fig. 3.

observed (Figs 2 and 3) to vary somewhat in thickness. The titanium-alloy matrix consists of two phases α and β; the latter is known to be more reactive with the fibre material than the former. A microstructure of alternating α- and β-grains would thus be expected to react unevenly with the coated monofilament.

Figs 2b and 3b both show low-contrast fringes on the SiC side of the fibre–matrix interface. These are consistent with interference between Rayleigh waves excited in the SiC at negative defocus and partial reflections of these waves from the interface. Measurement of the fringe spacing implies a Rayleigh-wave velocity of $6325\,m\,s^{-1}$, which is less than the $6729\,m\,s^{-1}$ that was measured for monolithic SiC. It is however appreciably larger than the value ($5150\,m\,s^{-1}$) for the Tyranno SiC fibres reported in Part II [5]. That the value for the SCS-6 monofilament should lie between the values for the much smaller Tyranno fibre (diameter 9 μm) and for bulk material is reasonable. Using the same reasoning as in Part II, and assuming a density of $3045\,kg\,m^{-3}$ and a Poisson's ratio of 0.2, a shear modulus of 147 GPa and a Young's modulus of 352 GPa are deduced for the Textron SCS-6 monofilament SiC. The latter is lower than the value quoted for Young's modulus for Textron SiC monofilaments, 400–415 GPa, by about 12% – a similar variation to that reported for sigma-SiC monofilaments and Tyranno fibres in Part II.

Turning briefly to the material with the Ti_3Al matrix, it was found that the general appearance of the SiC monofilaments in the acoustic microscope was very similar to those in specimen 1 examined above. The same features were all clearly observed: a carbon core, a pyrolitic graphite layer and a mid-radius boundary. However, the fibre–matrix interface (Fig. 5) is different in appearance from Fig. 3. The interfacial region is more uniform in this material than in the composite with the Ti–6Al–4V matrix. Furthermore, differences in contrast are evident, suggesting differences in the composition of the various layers identified. This observation is consistent with Yang and Jeng [12] who examined the reaction layer and found it consisted of two sub-layers of complex titanium carbides and silicides. As with some of the Ti–6Al–4V matrix specimens, cracks (i.e. diffusion debonds) were observed between closely-spaced monofilaments. Certain cracks appeared to initiate at the interface between the inner and outer carbon-rich layers. Other shorter cracks were observed to traverse the reaction layer. These latter are believed to be due to thermal contraction stresses following fabrication.

Examination of the Al6061/SiC material in the acoustic microscope revealed few differences in the microstructure of the monofilaments themselves. However it was observed that the thickness of the remaining carbon-rich layer was less than in the titanium-based materials, which is indicative of greater reaction with the matrix. There were no defects between closely-spaced monofilaments in this material, undoubtedly because this material had been produced by melt infiltration rather than the diffusion bonding of foils.

3.2. Heat treated material

Low-power optical and acoustic microscopy reveal two main effects of heat treatment: loss of carbon cores and fibre bunching [10]. While there are no missing cores in either specimen 1 (as-fabricated) or specimen 2 (500 h at 450 °C), specimen 3 has lost some of its cores, and specimens 4 and 5 (the highest temperatures) have lost all their cores due to oxidation of the carbon. This oxidation of carbon cores (and the carbon-rich-monofilament coatings) may place a restriction on the use of this type of material unless oxygen-diffusion-inhibiting coatings are used on the outer surface. Bunching of the fibres is observed in all the heat-treated specimens, which appears to be associated with the formation of defects as discussed below.

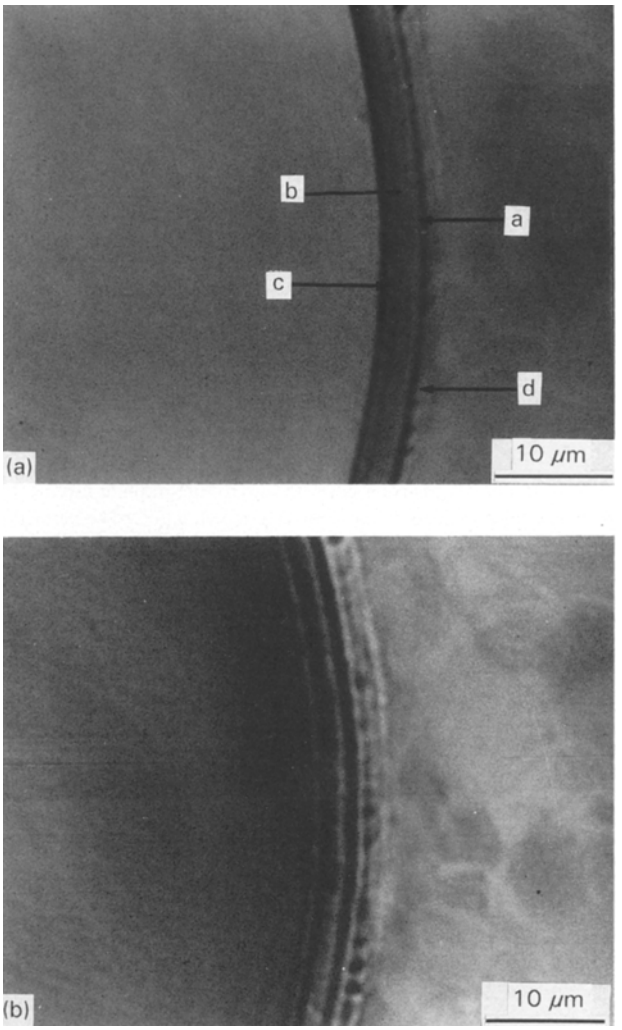

Figure 5 High-magnification acoustic image (1.9 GHz) of the interfacial region between the Ti_3Al matrix and the SiC monofilament at: (a) $z = 0$ μm, and (b) $z = -2.1$ μm. The arrows indicate: a an outer carbon-rich layer; b a silicon-rich carbon layer; c an inner carbon-rich layer; and d, a fibre–matrix reaction layer.

Fig. 6 enables the general features of the monofilaments and interfaces to be compared as a function of heat treatment. Each specimen still exhibits the same change of microstructure at the mid-radius, from finer to coarser SiC grains as in the as-fabricated material. However, all four heat-treated materials show a new feature in the form of an annular band at the mid-radius that was not observed in the as-fabricated material (Fig. 2). The annulus was consistently 6–7 μm wide, and can be seen most clearly in Fig. 6a and d. This annulus corresponds to the change in monofilament structure and composition observed in

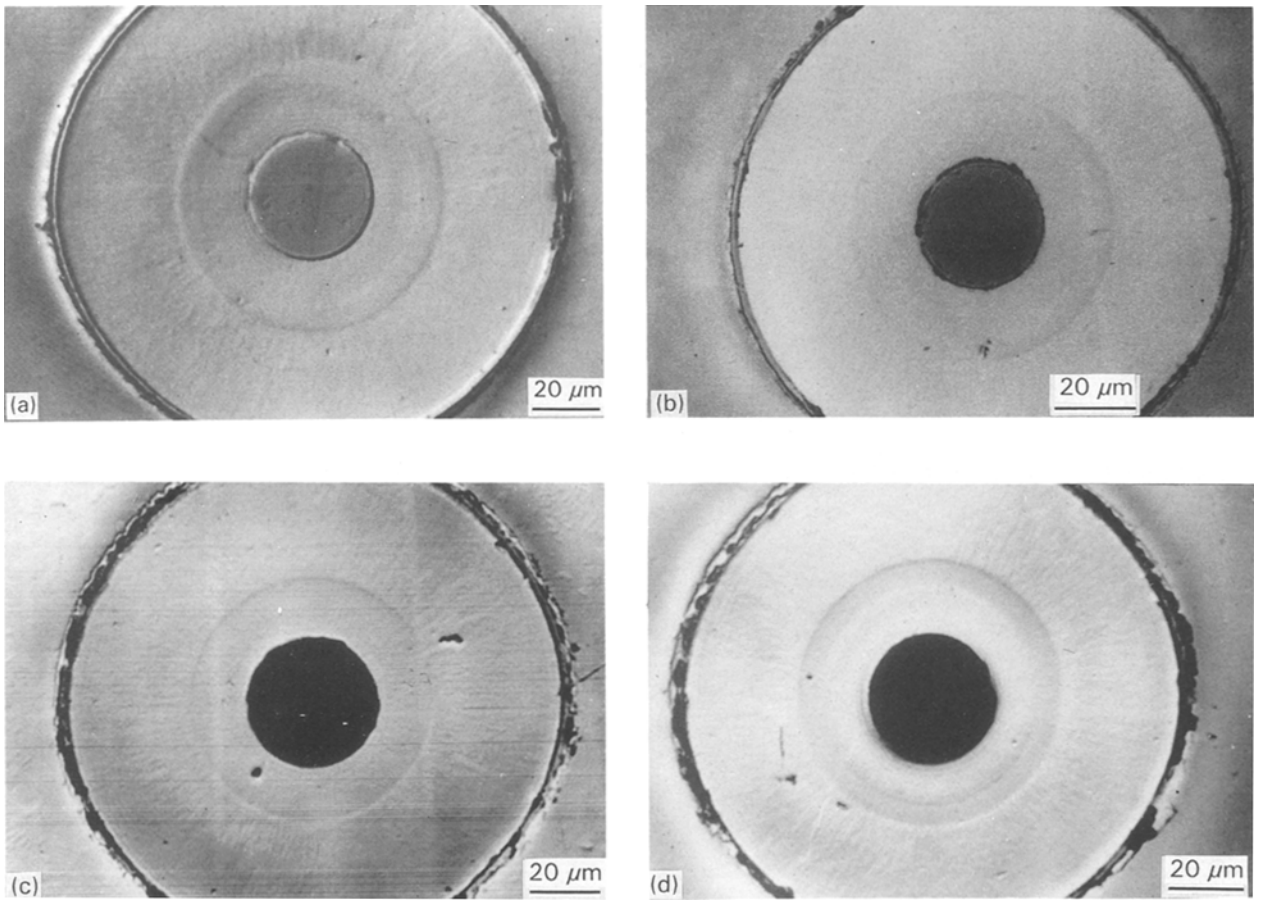

Figure 6 Acoustic micrographs (1.9 GHz, and $z = 0$ μm) of typical monofilaments in thermally aged material: (a) specimen 2, (b) specimen 3, (c) specimen 4, and (d) specimen 5. Compare with the as-fabricated material (Fig. 2).

as-fabricated monofilaments by Ning and Pirouz [13]. They found two SiC sublayers, each approximately 4.5 μm wide, to have formed at the point at which the annular structure was observed by the authors. Ning and Pirouz found that the inner of the two SiC sublayers showed an elongation and alignment of SiC grains, and the SiC grains in the outer sublayer had lengths of the order of micrometres and were heavily faulted. On crossing the sublayers, the composition of the monofilament changed from approximately 10–20% excess carbon to stoichiometric SiC. Ning and Pirouz speculated that the excess carbon was present at the SiC-grain boundaries. As the annulus was observable by the acoustic microscope only in heat-treated specimens, it can be concluded that the heat treatment resulted in preferential growth of the SiC grains in this region.

Increasingly harsh heat treatments result in progressive deterioration of the interface between the fibres and the titanium-alloy matrix (Fig. 7). The reaction layer in the as-fabricated specimen 1 only varied slightly in thickness as a result of differences between α- and β-titanium grains (Fig. 2). Specimen 2 is markedly different (Fig. 7a), the reaction layer between the fibre and matrix being variable in thickness. Fig. 7a is taken at focus so that the contrast variations in the interfacial region are mainly due to variations in acoustic impedance rather than to interference fringes. Thus the contrast variations observed must be due to a more complex structure than in the as-fabricated material. The inner continuous layer that appears grey in Fig. 7a has a thickness of 1.4 μm and therefore corresponds to the inner layer of the original carbon-rich coating.

Outside this layer there is a discontinuous "crenellated" layer up to 1.5 μm thick which is lighter in contrast (Fig. 7a). Since Fig. 7a was taken at focus this implies a higher acoustic impedance, i.e. greater density and/or a higher elastic modulus. The length of the crenellations corresponds approximately to the size of the matrix grains, which are revealed at negative defocus in Fig. 7b. This suggests that parts of this outside layer have been consumed in a reaction with certain grains in the matrix. It would thus be consistent with the higher reactivity of the β-phase Ti grains. Between the crenellated layer and the matrix is a dark line, but the resolution is insufficient to determine whether this signifies reduced bonding or the presence of remnant carbon. There are further contrast variations in the matrix, this could possibly be due to the presence of TiO_2 or TiC.

Further changes to the fibre–matrix interface are observed (Fig. 7c) in specimen 3, indicative of further degradation compared to specimen 2. Thus the inner remaining carbon-rich layer is no longer present, having been replaced by a narrow dark region indicating a much lower acoustic impedance such as would be caused by a narrow gap. It is possible that the inner

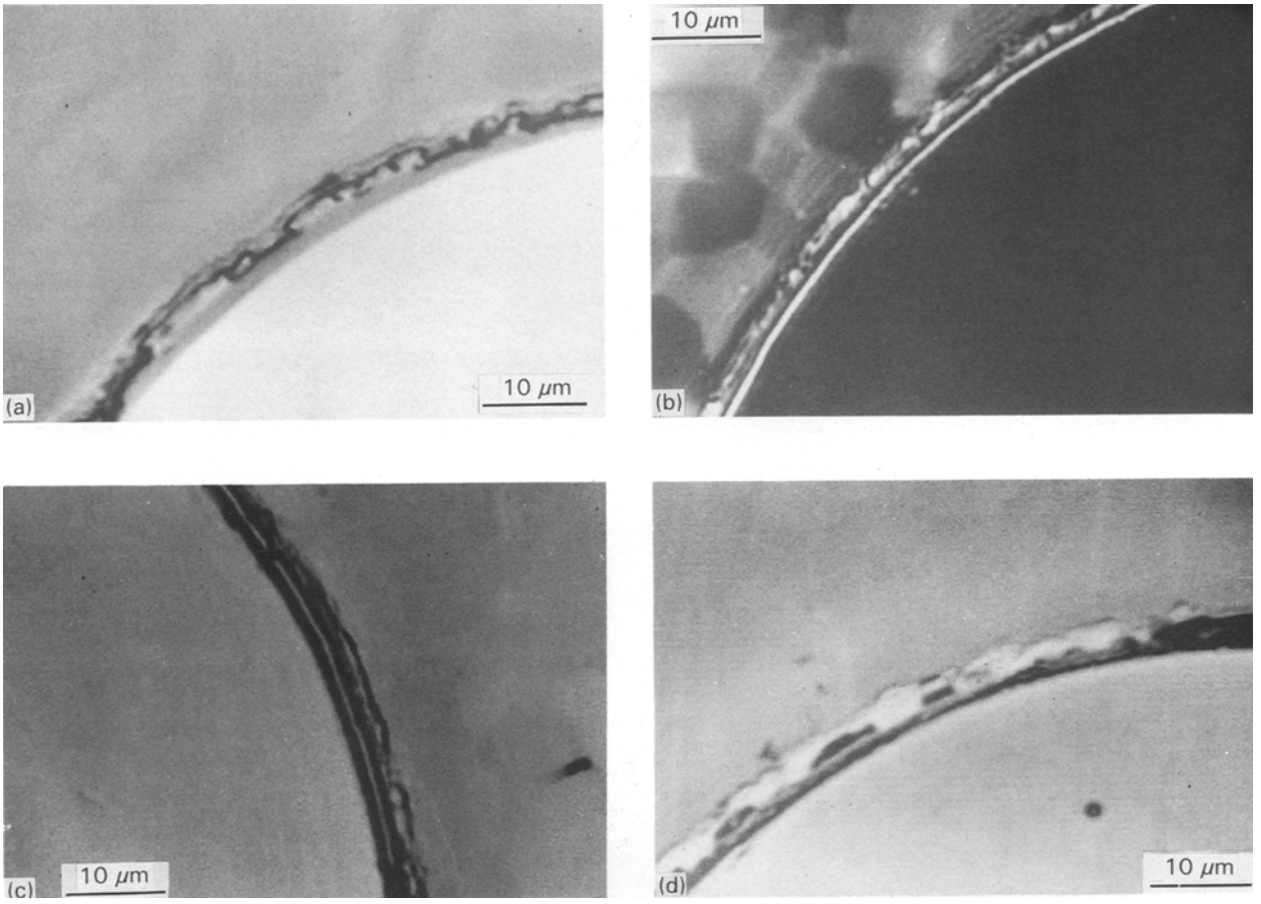

Figure 7 Higher-magnification acoustic images (1.9 GHz) of the interfacial region in thermally aged material: (a) specimen 2 at $z = 0$ μm, (b) specimen 2 at $z = -2.1$ μm, (c) specimen 3 at $z = 0$ μm, and (d) specimen 4 at $z = 0$ μm.

TABLE II Interfacial structures in Ti–6Al–4V as a function of thermal ageing

Specimen	Inner carbon layer (μm)	Outer carbon layer (μm)	Reaction layer (μm)	Reaction layer composition
1	1.4	1.0–1.3	0.2–0.7	TiC + Ti silicide
2	1.5	0.0–1.5	0.2–1.3	TiO_2 + TiC + Ti silicide
3	1.5	0[a]	1.5	TiO_2 + some TiC
4	1.5	0[a]	1.0–2.0	TiO_2 + trace TiC
5	1.5	0[a]	2.0–2.5	TiO_2

[a] Denotes that the layer has been totally consumed.

carbon-rich layer had deteriorated to such an extent that it was easily damaged and removed during the polishing of the specimen. Some form of light-coloured reaction layer is still observed, varying in thickness from 1–1.5 μm. However, Fig. 7c shows that in specimen 3 there is also discrete damage to the SiC fibre material itself, which takes the form of notches or pores.

More extensive degradation of this interface was observed in specimens 4 and 5. In Fig. 7d a light-contrast reaction layer is present, but here it is both intermittent and thicker (3 μm) than previously. The reaction layer is believed to be mainly composed of TiO_2. There are much greater dark regions which indicate absence of material and porosity. Some of the porosity could have developed as the reaction layer degraded at 600 °C. Alternatively, the reaction layer was very weak so that it was easily damaged during specimen preparation.

The changes that occur to the layers on the fibre–matrix interface are summarized in Table II. It can be seen that the outer carbon-rich layer is rapidly consumed during prolonged thermal ageing, as a progressively thicker reaction layer is simultaneously formed. The composition of this reaction layer, as determined using energy-dispersive spectroscopy (EDS), changes progressively from being mainly TiC (with Ti_5Si_3 and/or Ti_3SiC_2) to mainly TiO_2. Note that the inner carbon layer mainly remains intact, continuing to protect the SiC monofilament; although, as noted above, some discrete defects do form to penetrate this layer in, for instance, specimen 3 (Fig. 7c).

The bunching of the fibres that is observed in the heat-treated materials is accompanied by defect formation in the matrix, which is a result of the composite-fabrication process [14]. The first type of defect (Fig. 8a) consists of a fine crack which joins up

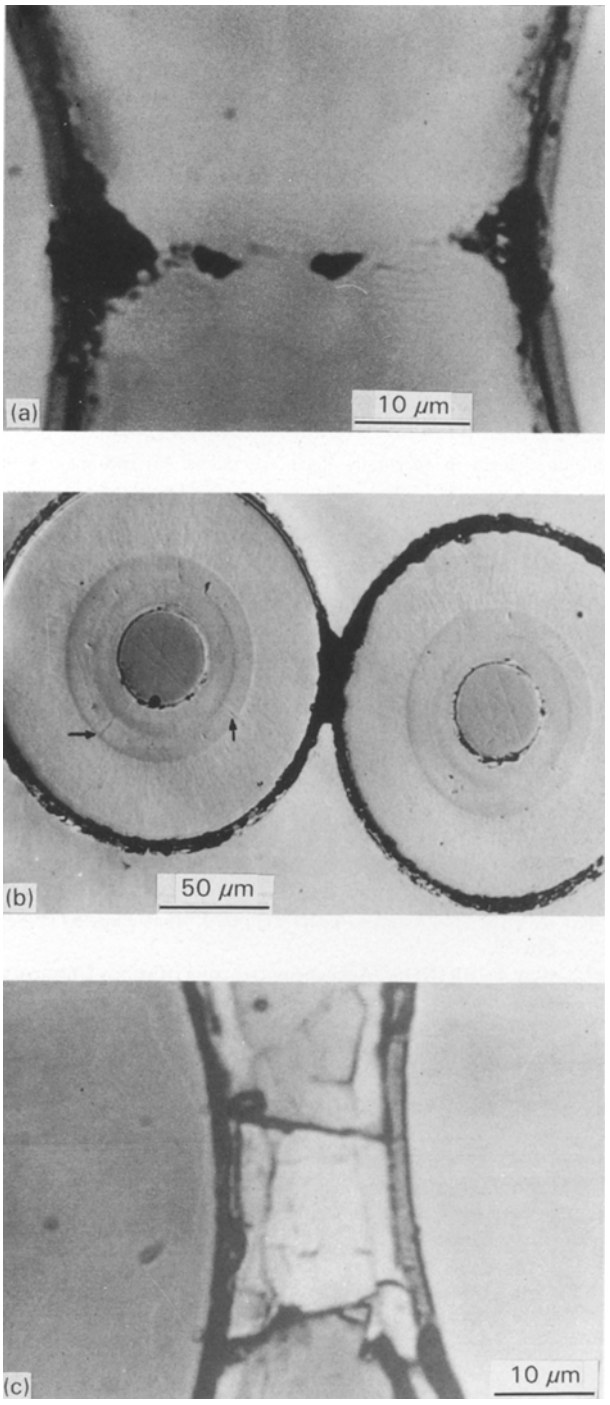

Figure 8 Fabrication defects observed acoustically (1.9 GHz) in thermally aged material: (a) crack due to poor diffusion bonding in specimen 2 ($z = 0$ μm), (b) porous void between bunched fibres in specimen 4 ($z = 0$ μm), the arrows indicate radial microcracking; and (c) cracks in the reaction layer joining adjacent fibres ($z = -1.0$ μm).

regions of porosity at the fibre–matrix interface in adjacent fibres. The crack was invisible in the optical microscope but made visible acoustically by the presence of Rayleigh-wave fringes either side. The nature and geometry of this type of defect suggests its formation during fabrication, the close proximity (less than half a diameter) of two monofilaments preventing adjacent titanium foils from making a good diffusion bond. The second type of defect (Fig. 8b) consists of a porous region between two monofilaments that are too close for the titanium foils even to make contact. Whereas the second type of defect was observed in all the heat-treated materials, the first type was relatively rare, only occurring in specimen 2. An unusual type of defect was observed in specimen 5, where the interfacial TiO_2 reaction layer (formed during the heat treatment) extends between adjacent monofilaments. Fig. 8c shows that this region is traversed by two distinct cracks. They do not, however, appear to cross the inner interfacial layer of the right monofilament, suggesting that it is the residual carbon-rich-coating layer.

All heat treatments except the lowest were observed to induce radial microcracks in the annular-banded region of the SiC monofilaments (Figs 9a, 8b and 9b), 23%, 9% and 31% respectively of the monofilaments were microcracked in specimens 3, 4 and 5. Specimens 3 and 5 (the longest heat treatments) also had the largest numbers of the second type of matrix defect discussed above. The microcracks in the monofilaments could not be observed by optical microscopy, indicating that they were very tightly closed, their acoustic contrast being enhanced by Rayleigh-wave fringes. They were often associated with bunched groups of monofilaments and porosity, which must cause concentrations of stress and strain, and it is postulated that these cracks formed as a result of stress relief during or immediately following the heat treatments.

4. Conclusion

The main conclusions of this study concern the effects of heat treatment on the integrity of the composite. Some deterioration was observed by acoustic microscopy for the minimum treatment studied of 500 h at 450 °C. Raising the ageing temperature or extending the ageing time both cause further progressive deterioration of the fibre–matrix interface. In the as-received material the carbon-rich coating protected the SiC by forming a reaction layer with the titanium. During ageing, the reaction layer was first penetrated mainly adjacent to the β-titanium grains. This enabled the carbon-rich coating to degrade and eventually disappear. The final stage in observed deterioration took the form of direct attack on the SiC material of the monofilament.

The second major observation was the presence of defects in both matrix and monofilaments. These fell into two categories. The defects in the matrix, i.e. cracks and porosity between monofilaments, were most probably generated during fabrication, and linked with bunching of the monofilaments and hence poor diffusion bonding between adjacent metal foils. Although the monofilament bunching must itself have occurred during fabrication, the heat treatments could well have increased the associated defect severity. However, the fine radial microcracks that were observed to develop in the annular region inside the mid-radius of the monofilaments in specimens 3–5 are believed to be a direct result of thermal ageing. Their appearance suggests that they formed to relieve tensile hoop stress in the SiC at high temperatures.

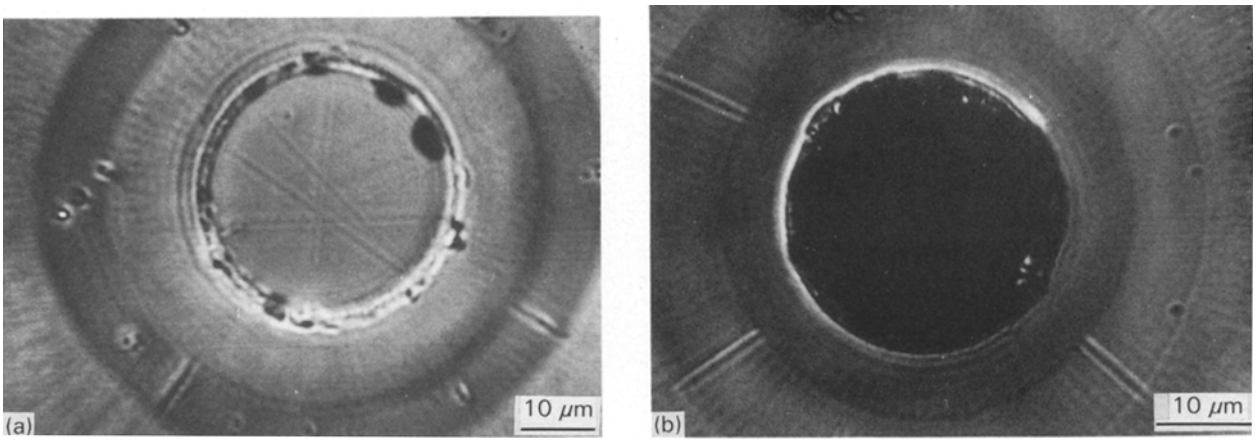

Figure 9 Examples of acoustic images (1.9 GHz) of radial microcracking defects in thermally aged specimens: (a) specimen 3 at $z = -2.0$ μm, and (b) specimen 5 at $z = -2.5$ μm.

Finally, this study has illustrated how acoustic microscopy can provide fresh insights into the microstructural changes that accompany the thermal ageing of MMCs. Thus, the radial microcracks that formed in the SiC monofilaments as a result of heat treatment could not be observed by optical microscopy. The extra sensitivity of the acoustic images arises because Rayleigh waves still undergo appreciable reflection from tight cracks. Furthermore, the degradation of the carbon-rich layer at the fibre–matrix interface could be monitored more sensitively by acoustic microscopy because the microstructural changes caused larger variations in acoustic properties (which control image contrast) than in optical reflectivity.

Acknowledgements

The authors thank M. Hartley (Rolls–Royce Plc, Derby) and M. A. Mittnick (Textron Speciality Materials, Massachusetts) for the supply of specimens. CWL was supported by a SERC quota award and CBS by the Corporate Research Programme of AEA Technology. The use of the ELSAM at Oxford is in collaboration with Leica, Wetzlar; and we particularly wish to thank Mr K. Krämer of Leica.

References

1. M. TAYA and R. I. ARSENAULT, in "Metal matrix composites: Thermo-mechanical behaviour" (Pergamon Press, Oxford, 1989).
2. J. A. McELMAN, in "Engineering materials handbook: Composites", Vol 1, (American Society for Metals, Metals Park, Ohio, 1987) 858–66.
3. J. C. ROMINE, "Engineering materials handbook: Composites", Vol 1 (American Society for Metals, Metals Park, Ohio, 1987) 874–7.
4. C. W. LAWRENCE, C. B. SCRUBY, G. A. D. BRIGGS and J. R. R. DAVIES, *J. Mater. Sci.* **28** (1993) 3635.
5. C. W. LAWRENCE, G. A. D. BRIGGS and C. B. SCRUBY, *J. Mater. Sci.* **28** (1993) 3645.
6. K. YAMANKA and Y. ENOMOTO, *J. Appl. Phys.* **53** (1982) 846–50.
7. G. A. D. BRIGGS, "Acoustic microscopy" (Oxford University Press, Oxford, 1992).
8. C. B. SCRUBY, C. W. LAWRENCE, D. G. FATKIN, G. A. D. BRIGGS, A. DUNHILL, A. E. GEE and C-L. CHAO, *Brit. Ceram. Trans. J.* **88** (1989) 127–32.
9. J. KUSHIBIKI, A. OHKUBO and N. CHUBACHI, *Elect. Lett.* **17** (1981) 520–22.
10. C. W. LAWRENCE, D Phil. thesis, University of Oxford, Oxford (1990).
11. C. JONES, C. J. KIELY and S. S. WANG, *J. Mater. Res.* **4** (1989) 327–35.
12. J. M. YANG and S. M. YENG, *Scripta. Metall.* **23** (1989) 1559–64.
13. X. J. NING and P. PIROUZ, *J. Mater. Res.* **6** (1991) 2234–48
14. X. GUO and B. DERBY, submitted to *J. Micro.*

Received 11 September
and accepted 10 December 1992